Salinity distribution analysis for the region of freshwater influence (RoFI) at the Musi-Banyuasin Estuary, Indonesia

Muh. Adhim Adrian[1], *I Wayan* Nurjaya[1*], *Dietriech Geoffrey* Bengen[1], *Jonson Lumban* Gaol[1] and *Heron* Surbakti[2]

[1]Department of Marine Science and Technology, Faculty of Fisheries and Marine Sciences, IPB University, Bogor, Indonesia
[2]Department of Marine Science, Faculty of Mathematics and Natural Sciences, Universitas Sriwijaya, Indralaya, South Sumatra, Indonesia

Abstract. RoFI is a transition zone where fresh water and sea water mix, characterized by water column stratification, with salinity as the key parameter. This study is the first to identify RoFI based on salinity gradients in the Musi–Banyuasin Estuary, aiming to reveal the distribution patterns of salinity and oceanographic parameters that influence RoFI extent. Observations were conducted at 9 stations using CTD, with horizontal and vertical profiles visualized in ODV, and tides and currents analyzed as the primary controllers of RoFI dynamics. The results show that RoFI can be clearly identified through salinity distribution, where the Musi Estuary is characterized by low surface salinity (5 PSU) and water column salinity of 25–30 PSU at high tide, with residual freshwater influence at low tide, while the Banyuasin Estuary is dominated by high salinity (24–28 PSU) throughout the water column, reflecting the dominance of seawater. PCA analysis (80.41%) confirmed that the RoFI area is closely related to tides, currents, and river discharge. However, the limited observation period indicates the need for further season-based studies to understand RoFI dynamics better.

Keywords: RoFI, salinity, Musi–Banyuasin Estuary, tidal dynamics, seawater intrusion

1 Introduction

The Musi-Banyuasin Estuary is one of the largest estuarine systems in eastern Sumatra, located approximately 72 km from the city of Palembang [1]. This area is strongly influenced by the flow of the Musi River and its tributaries, which discharges substantial volumes of freshwater into the sea. The region's low-lying topography allows tidal water to intrude far upstream, with hydrodynamic conditions predominantly driven by tidal fluctuation [2, 3].

*Corresponding author: i.wayan.nurjaya@apps.ipb.ac.id

© The Authors, published by EDP Sciences. This is an open access article distributed under the terms of the Creative Commons Attribution License 4.0 (https://creativecommons.org/licenses/by/4.0/).

The Banyuasin and Musi estuaries exhibited distinct characteristics in terms of water mass transport. The Banyuasin Estuary carries a larger volume of low-salinity water from upstream to the sea than the Musi Estuary, which displays pronounced daily variability and a limited freshwater input [4]. These variations in water density result in vertical stratification, where the freshwater layer remains on the surface with minimal mixing with the underlying saltwater layer [5].

The water mass dynamics in both estuaries were largely influenced by hydrodynamic shifts driven by anthropogenic activities and climate variability. In the lower reaches of the Musi River, where it converges with the Yangtze River, the average flow rate is approximately 2,500 m^3/s, ranging from 1,400 m^3/s during the dry season to 4,200 m^3/s during the rainy season. The significant volume of freshwater discharged by the Musi-Banyuasin River system forms a Region of Freshwater Influence (RoFI), a coastal zone where river water mixes with seawater [6]. The extent of this RoFI can range from several to hundreds of kilometers from the river mouth, depending on the river discharge and various environmental factors [7].

Although RoFI systems have been extensively studied in several coastal regions worldwide [8, 9], such research in Indonesia remains limited, particularly in the Musi-Banyuasin Estuary. RoFI represents a complex physical environment in which the interaction between freshwater and seawater is modulated by multiple variables including wind speed, tides, estuarine morphology, and river discharge [10]. The conceptual model of RoFI, in which freshwater exits the river mouth under weak wind conditions, is divided into two main components [11]. The first is a baroclinic recirculation bulge near the mouth, where freshwater accumulates and circulates prior to spreading. The second is a coastal current that carries freshwater along its shoreline. In the absence of external forces such as ocean currents or wind, this bulge can expand continuously and circulate anticyclonically. However, strong external forces such as wind events or offshore currents can alter the flow pattern [12].

Several studies have demonstrated a correlation between increased freshwater discharge and salinity distribution in estuarine environments [13]. Other studies have identified turbidity fronts using two-dimensional modeling and Landsat 8 imagery [14]. While the dominance of the Musi River freshwater input and its tidal interactions has been addressed in prior studies, the specific interaction between these processes within the RoFI zone of the Banyuasin Estuary has yet to be thoroughly examined, highlighting the novelty of this research.

This study aimed to identify salinity distribution patterns and analyze the oceanographic parameters that significantly influence the spatial extent of the RoFI in the Musi-Banyuasin Estuary. A comprehensive understanding of the RoFI dynamics is essential for predicting coastal primary productivity, which directly affects phytoplankton growth and food web dynamics. This study provides critical insights for effective coastal zone management. This study presents the first RoFI investigation in the Musi-Banyuasin Estuary, specifically examining the salinity distribution both vertically and horizontally. The Principal component analysis (PCA) approach serves as a key analytical tool for identifying the parameters that contribute to the RoFI characterization.

2 Materials and methods

2.1 Study site

This study was conducted in the waters of the Banyuasin Estuary, South Sumatra, Indonesia (**Fig. 1**) with a field study period from August 14 to 18, 2024. The study area is bounded by the Banyuasin and Musi Rivers, as well as the waters of the Bangka Strait.

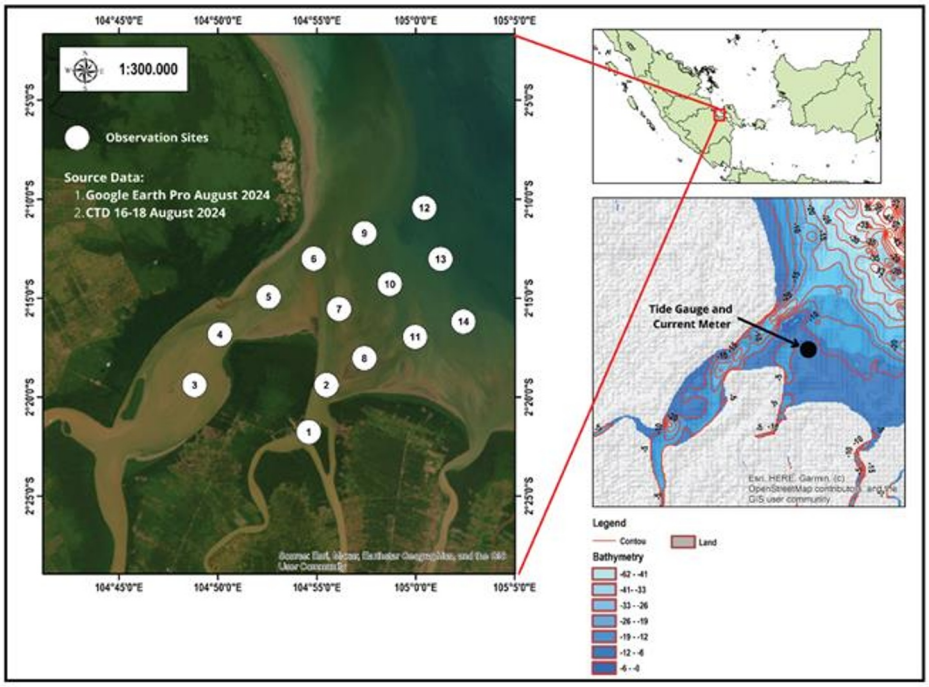

Fig. 1. Research location map. CTD points (white circles) were placed along the estuary at 14 points. Tide gauges and current meters (black circles) were placed near station 11.

2.2 Data collection

Tidal fluctuations were recorded over a three-day period from August 16 to 18, 2024, using a tide gauge installed at a strategic location that remained submerged even during the lowest tide. The current speed and direction were measured using a current meter and the device was carefully positioned based on tidal conditions to ensure the accuracy of the data. Special attention was paid to the sensors to maintain the quality and reliability of the recorded measurements.

Water quality parameters, including temperature, salinity, dissolved oxygen, and turbidity, were measured using a RINKO-Profiler CTD sensor known for its fast response time (0.4 s). Measurements were conducted at 14 stations distributed across the Musi and Banyuasin estuaries to capture the spatial variability and assess the influence of tidal dynamics on water characteristics. The river discharge data were obtained from the openly accessible GLOFASS website.

2.3 Colour illustrations

Tidal and current data were collected and processed using MATLAB software. The salinity distribution was analyzed using Ocean Data View version 5.8.1 (2025), generating both vertical visualizations. Statistical analysis was conducted by Principal Component Analysis (PCA) using XLSTAT software.

2.4 Data analysis

2.4.1 Analysis of current speed and direction

In-situ measurements using a current meter revealed that the current speed and direction varied in accordance with the tidal cycle. During the flood tide, the current generally flowed upstream, whereas during the ebb tide, it shifted toward the estuary. The highest velocity was recorded during the transition phase between the flood and ebb, confirming that fluctuations in sea level directly influence the intensity of the current movement within the estuary. Furthermore, the current data were processed and visualized as a current vector diagram to provide a more comprehensive depiction of the flow patterns, complemented by a current rose to represent the dominant current directions [15].

2.4.2 Tidal analysis

Tidal measurements were conducted over a three-day period, from August 16 to 18, 2024. The observations indicated that on August 16, the tide was in an ebb phase, whereas on August 18, it was in a flood phase, with relatively stable tidal elevations throughout the period. The data show that the time required to reach high tide was approximately 8–9 h, whereas the time to reach the lowest low tide ranged from 12 to 14 h. These results are consistent with the findings of, who reported that, in the Musi Estuary, the duration of seawater inflow was shorter than the outflow period. The classification of tidal type was determined using the Formzahl number, calculated based on the following equation proposed by [16]:

$$F = \frac{O1+K1}{M2+S2} \quad (1)$$

The Formzahl (F), a critical tidal form factor, was calculated to quantify the relative significance of the diurnal and semidiurnal tidal components. Mathematically, the F value is derived from the ratio of the summed amplitudes of the two principal diurnal constituents, K1 (diurnal lunisolar tide) and O (diurnal primary lunar tide), to the summed amplitudes of the two principal semidiurnal constituents, M2 (principal lunar tide) and S2 (principal solar tide). This ratio establishes a key metric for classifying the tidal regime at a specific location. The Formzahl categories are presented in **Table 1**.

Table 1. Classification of tidal types based on the formzahl number (F).

Formzahl number	Tidal type	Description
$0 < F \leq 0.25$	Semidiurnal	Two high tides and two low tides in a day
$0.25 < F \leq 1.5$	Mixed tide prevailing Semidiurnal	Two high tides and two low tides in a day with different heights and periods. Occasionally, there is only one high tide and one low tide
$1.5 < F \leq 3$	Mixed tide prevailing Diurnal	One high tide and one low tide in a day. Occasionally, there are two high tides and two low tides with different heights and periods
$F > 3$	Diurnal	One high tide and one low tide in a day

Table 1 presents the classification of tidal types based on the Forzahl (F) number, which was used to determine the frequency of tides occurring in a day. This range of values divides tidal types into four categories: semidiurnal (two tides with almost equal heights), mixed tide prevailing semidiurnal, mixed tide prevailing diurnal, and diurnal, with only one high tide and one low tide per day. This information is very important in coastal dynamics analysis

because it helps predict the characteristics of water mass movement and timing of tidal phenomena in a region.

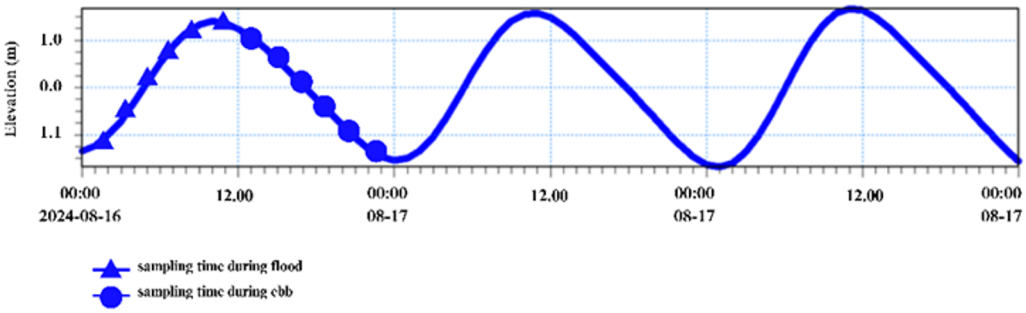

Fig. 2. Sea level elevation over time showing the sampling schedule during the tidal cycle at the research site on August 16–17, 2024.

2.4.3 Principal component analysis (PCA)

PCA was used in this study to assess the relationship between ocean dynamics and the physical and chemical parameters of seawater. This analysis was performed using the XLSTAT 2019 3.2 software integrated with Microsoft Excel to facilitate the visualization of PCA results through biplots and factor matrices.

3 Results and discussion

3.1 Morphology of the Musi-Banyuasin Estuary

The water masses entering the Musi-Banyuasin Estuary originate from several tributaries that flow into both river systems. Based on the geomorphological characteristics, clear differences can be observed in the catchment area and length of each main river, as well as in the number and contribution of their tributaries. These factors play a significant role in determining the volume of freshwater discharge received by each estuary [17].

The Musi River estuary is generally characterized by relatively shallow bathymetric conditions compared with the Banyuasin River estuary. This is likely attributable to the high intensity of anthropogenic activities in the area, including barge shipping routes and industrial operations [18]. Additionally, the elevated sedimentation rate contributes to the accumulation of suspended particles, resulting in higher turbidity in the Musi River throughout the year than in the Banyuasin Estuary [19].

In contrast, the Banyuasin River Estuary exhibits deeper bathymetric features, particularly in the middle to lower reaches. It also possesses a longer and wider morphology than that of the Musi River, making it more susceptible to seawater intrusion. Consequently, the residence time of the water masses in this estuary is relatively longer, and the flushing process occurs more slowly, especially between the maximum high and low tide phases. Furthermore, the Banyuasin River generally delivers smaller freshwater discharge than the Musi River, leading to a relatively lower fraction of freshwater in the Banyuasin Estuary.

Fig. 3. Spatial morphology of the Banyuasin and Musi River Estuary. This map displays critical dimensions and bathymetric contours of the river systems, including the 25.40 km Banyuasin River stretch, to provide spatial context for hydrodynamic analysis.

3.2 Current speed and direction

Based on the in-situ current measurements presented in **Fig. 4,** the dynamics of currents in the estuary are strongly influenced by oceanic forcing, which in turn drives the inflow of seawater into the river mouth. This was reflected in the fluctuation pattern of the total current velocity, with a maximum alignment of approximately 0.2 m/s. Throughout the observation period, the total current consistently followed the tidal cycle, as evidenced by changes in both the current direction and intensity in response to changing tidal conditions. These findings highlight the dominant role of tides in shaping current characteristics within estuaries.

As illustrated in **Fig. 5**, the current rose diagram indicates that total currents were predominantly oriented north–south, with velocities ranging from 0.1 to over 0.4 m/s. The highest current proportion was recorded in the north, showing strong fluctuations, while the calm condition accounted for 16.93%. This dominant directional pattern reflects the strong influence of tidal forces aligned with the central axis of the estuary, which is reinforced by its north–south geomorphological orientation. The concentration of current energy along these two principal directions further suggests a characteristic bidirectional circulation system in which seawater enters and exits the estuary under the influence of strong tidal cycles [20].

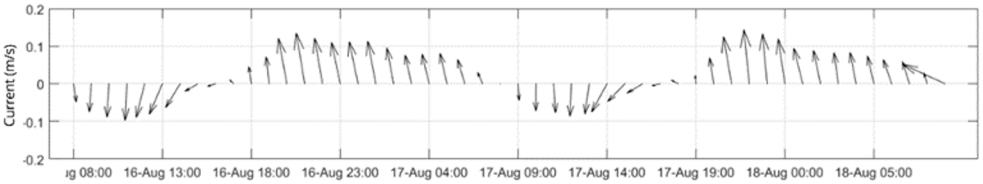

Fig. 4. Total current velocity measured in situ at Musi-Banyuasin Estuary, August 16–18, 2024. This vector plot illustrates the fluctuations in current speed and direction over a multi-day period, showing distinct patterns corresponding to ebb and flood tidal phases.

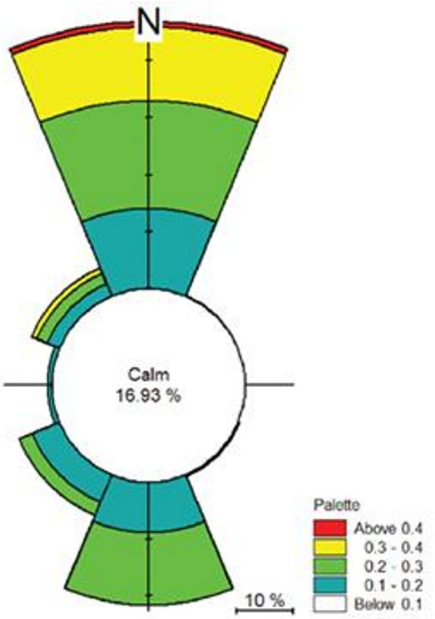

Fig. 5. Current roses in Musi-Banyuasin Estuary based on field measurements. The current rose illustrates the dominant orientations of water movement, showing a primary flow axis along the North-South direction, with a "Calm" period occurring 16.93% of the time.

3.3 River discharge in Musi-Banyuasin Estuary

Analysis of river discharge in the Musi-Banyuasin Estuary revealed substantial differences in flow patterns between the two rivers (**Fig. 6**). The Musi River demonstrates pronounced seasonal variability, with peak discharge reaching approximately 90 m^3/s in February, gradually declining to a minimum during August–September, and subsequently increasing toward the end of the year. In contrast, the Banyuasin River exhibits a relatively stable discharge throughout the year, ranging from 1 m $^3/s$ to 5 m^3/s, without clear seasonal fluctuations.

These differences were closely related to the morphological characteristics of the two estuaries. The Musi Estuary, located in the western part, is longer, narrower, and has a well-defined main channel with a few tributaries, resulting in a more restricted cross-sectional profile. Conversely, the Banyuasin Estuary exhibits a more complex morphology, characterized by multiple tributary branches, including the Telang River, Sri Menanti River, and Saleh River. Its main channel widened before discharging into the Bangka Strait, resulting in a more open estuarine system [21].

Overall, the discharge analysis indicates that the Musi River serves as the primary freshwater contributor to the estuarine region, whereas the Banyuasin River plays a comparatively minor role. The higher Musi discharge during the early months corresponds to the rainy season in the upstream catchment, whereas the mid-year decline reflects the dry season conditions. These contrasting discharge regimes emphasize the dominant role of the Musi River in regulating estuarine oceanographic dynamics, particularly with respect to the salinity distribution, suspended sediment transport, and water column stratification.

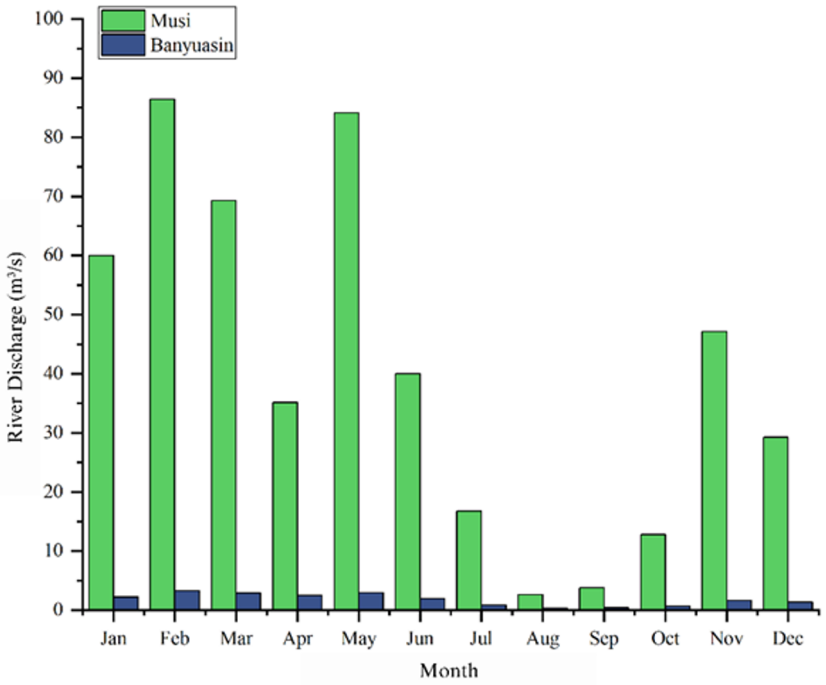

Fig. 6. Comparison of monthly river flow patterns of the Musi River (green) and Banyuasin River (blue) throughout 2024, illustrating differences in temporal variability that reflect different hydrological systems and their potential influence on estuary dynamics, during 2024.

3.4 Identification of RoFI conditions based on salinity of water

The vertical salinity profile of the Musi River Estuary (**Fig. 7**) shows distinct distributions under flood and ebb tide conditions. Salinity was measured along a transect from upstream to downstream, and across depths (0–10 m at flood tide and 0–5 m at ebb tide). During the flood tide, a clear salinity gradient was observed, with freshwater dominating the upstream surface layer (5 PSU), whereas salinity increased downstream, particularly in the bottom layer, reaching up to 25 PSU at depths greater than 5 m, indicating significant seawater intrusion. Conversely, during the ebb tide, seawater dominated nearly the entire water column from 5 km downstream, with salinity values approaching 30 PSU. Although traces of freshwater (20 PSU) were still detected at the upstream surface, their vertical extent was limited, suggesting that the upstream discharge was insufficient to counter seawater intrusion during ebb conditions. These results highlight the critical role of tidal forcing in shaping salinity stratification [22].

The stratification dynamics in the Musi River Estuary were strongly controlled by the interaction between upstream freshwater input and seawater intrusion. At flood tide, the convergence of these two water masses produced a thicker and more pronounced

stratification, whereas during ebb tide, the downstream water column became relatively homogeneous because of the dominance of seawater that was not fully displaced. This indicates that the salinity intrusion is stronger than it appears at the surface, particularly when freshwater input weakens during ebb conditions, reflecting the complex hydrodynamics of the estuary.

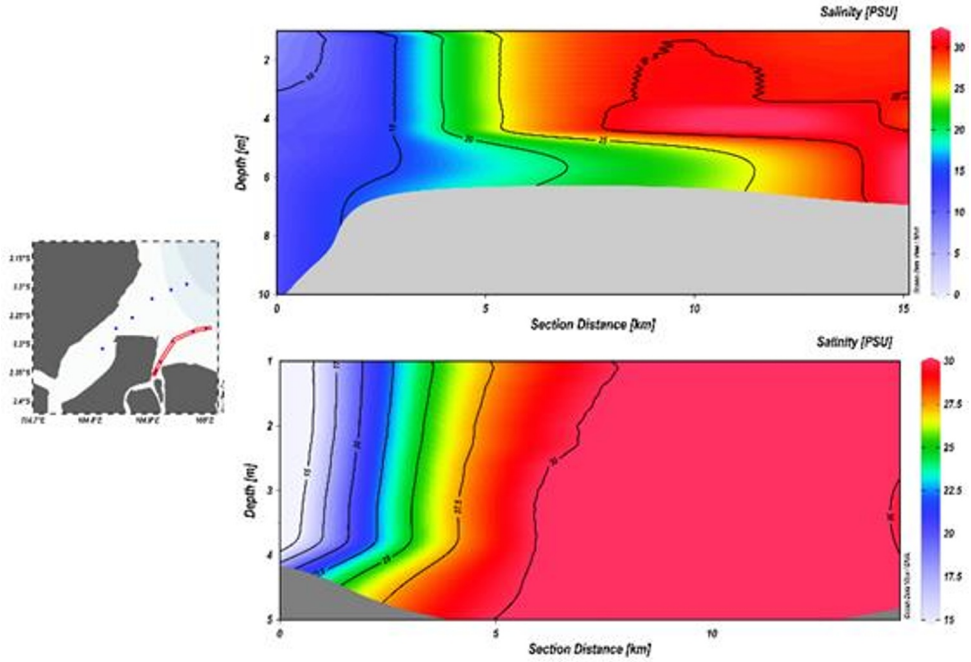

Fig. 7. Vertical salinity conditions at the Musi River estuary during a) flood tide and b) ebb tide. This cross-sectional visualization illustrates the stratification and saltwater wedge intrusion within the water column, where salinity values range from approximately 15 PSU (blue) to 30 PSU (red).

In contrast, the vertical salinity profile of the Banyuasin River Estuary (**Fig. 8**) revealed a different pattern. During the flood tide, relatively low salinity values (24–28 PSU) were recorded at the surface in the mid- to downstream transects, whereas higher salinity (30 PSU) occurred in the bottom layer due to seawater intrusion from the Bangka Strait. This produced a distinct vertical stratification, especially downstream, where the bottom seawater interacted with the surface freshwater, forming contrasting salinity layers. However, during ebb tide, stratification weakened substantially, and nearly the entire water column was dominated by high salinity (>30 PSU), particularly beyond 10 km upstream. The freshwater influence was minimal and detectable only near the upstream surface, with values still exceeding 28 PSU, underscoring the limited contribution of freshwater discharge. These results emphasize the stronger influence of seawater intrusion and the weaker role of freshwater input in shaping the salinity structure of the Banyuasin Estuary.

Analysis of the vertical salinity distribution in the Musi and Banyuasin River estuaries revealed notable differences in the physical characteristics of the water, which are closely linked to the dynamics of the Region of Freshwater Influence (RoFI). In the Musi River Estuary, the RoFI is well developed, with a freshwater surface layer extending downstream during flood tide and persisting, though weakened, during ebb tide. This condition is supported by the relatively high discharge of the Musi River, which is sufficient to counter seawater intrusion and to generate strong stratification in the water column. In contrast, RoFI is relatively limited in the Banyuasin River Estuary. The salinity distribution is dominated by

seawater intrusion throughout the water column, even during flood tide, indicating that the smaller freshwater discharge is insufficient to maintain a stable surface layer.

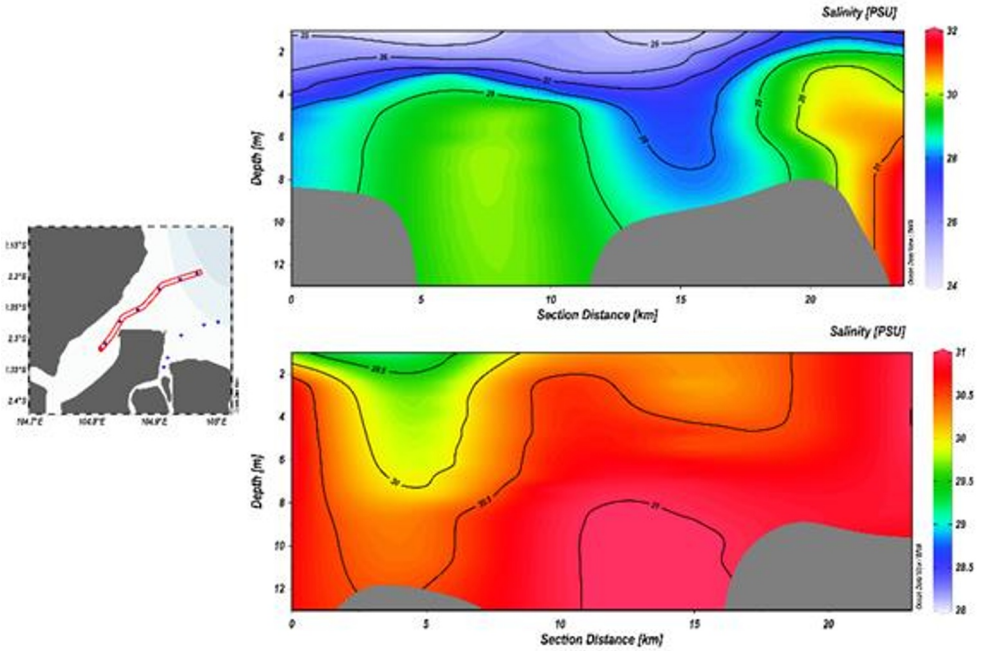

Fig. 8. Vertical salinity conditions at the Banyuasin River estuary during a) flood tide and b) ebb tide. This cross-sectional profile illustrates the vertical distribution of salinity across a 10–20 km section of the estuary, with values typically ranging from 24 PSU (blue) to 32 PSU (red).

These differences are influenced not only by river discharge but also by morphological and tidal dynamics. The Musi River Estuary, which has a long and narrow channel, enhances freshwater outflow, enabling it to displace downstream seawater masses and generate higher turbidity within the RoFI zone. Conversely, a wider and more branched Banyuasin Estuary facilitates more intensive seawater penetration, resulting in stronger vertical mixing. Combined with a tidal range of approximately ±3 m, seawater intrusion became dominant, rendering the RoFI in the Banyuasin Estuary relatively narrow and transient. Thus, the formation and persistence of the RoFI zone in both estuaries result from a complex interplay of freshwater discharge, estuarine morphology, and tidal forcing.

3.5 Distribution of oceanographic parameters in relation to RoFI conditions

Field observations at nine stations in the Musi-Banyuasin Estuary demonstrated that tidal dynamics play a crucial role in regulating the spatial and temporal variability of oceanographic parameters. Water temperature remained relatively stable between flood and ebb tides (29.0–30.1°C), although slight variations were detected at certain stations due to the intrusion of warmer surface water masses. More pronounced fluctuations were observed in salinity, which directly reflected the influence of seawater intrusion during the flood tide and the dominance of freshwater input during the ebb tide.

The salinity increased during the flood tide, ranging from 27.5 PSU upstream to 30.6 PSU at coastal stations, whereas during the ebb tide, it decreased significantly (24.3–27.5 PSU). This variation highlights the role of RoFI as a highly dynamic transition zone between freshwater and seawater. Changes in salinity were further associated with density and conductivity, both of which exhibited higher values during the flood tide and decreased

during the ebb tide. Thus, salinity has emerged as a key parameter for controlling the physical properties of estuarine water [23].

Other parameters also responded to the tidal fluctuations. Chlorophyll-a concentrations tend to rise during ebb tides, driven by nutrient inputs that stimulate phytoplankton growth [24]. Similarly, TSS and turbidity increased during ebb tide due to sediment resuspension and the dominance of outflow, while dissolved oxygen concentrations declined, likely as a result of biological consumption and decomposition of organic matter [25].

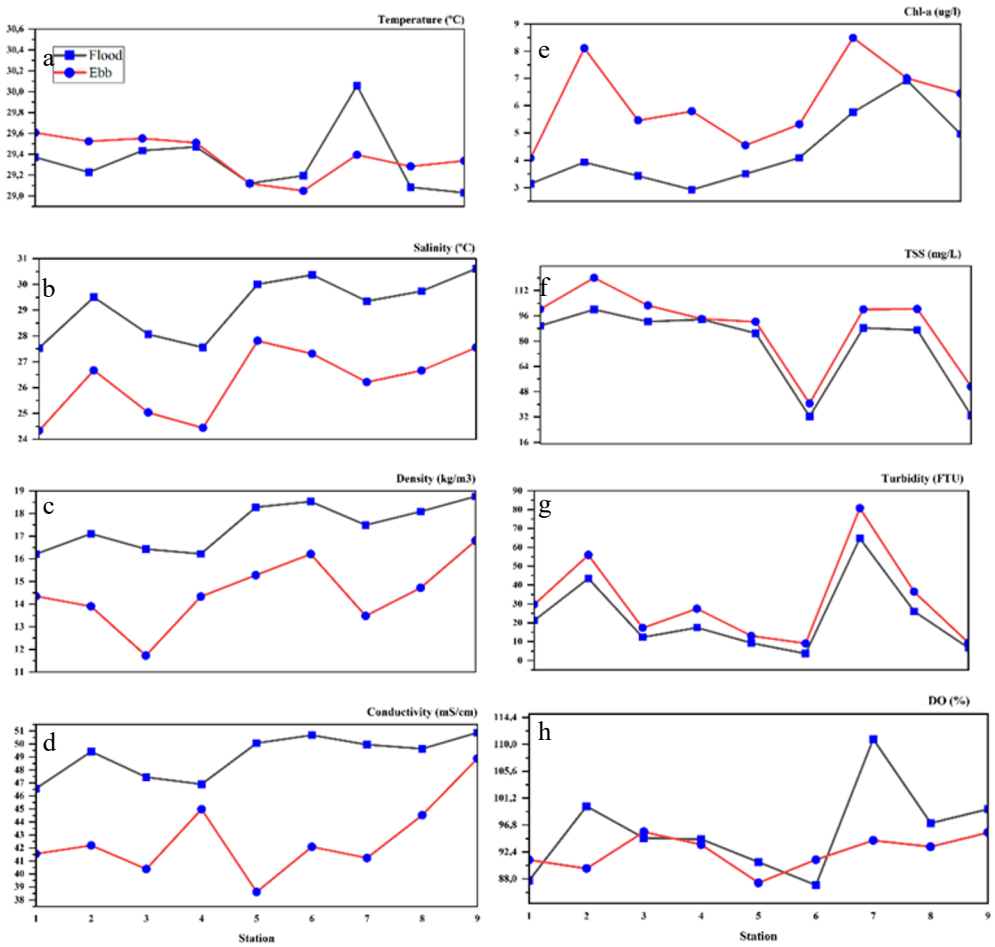

Fig. 9. Oceanographic parameters include a) temperature, b) salinity, c) density, d) conductivity, e) chlorophyll-a, f) TSS, g) turbidity, and h) DO at the time of high tide and low tide at the Musi-Banyuasin Estuary.

Based on the analysis of all parameters, it can be concluded that oceanographic dynamics in this region are predominantly controlled by tidal cycles, which affect the RoFI range. Flood conditions bring seawater masses characterized by high salinity, density, and conductivity, effectively suppressing the influence of freshwater at the observation stations. Conversely, during ebb conditions, the impact of river discharge becomes more dominant, reducing water salinity and density and carrying terrestrial material that increases turbidity and suspended solids in the water column.

From a biological and chemical perspective, ebb conditions play an essential role as a nutrient enrichment mechanism, triggering a significant increase in chlorophyll-a concentration compared to flood conditions. This indicates that primary productivity in this

estuary is highly dependent on the supply of organic and inorganic material from the land. Although the general pattern shows a transparent gradient, local fluctuations in temperature and dissolved oxygen parameters, particularly at the middle station, indicate complex water mixing or turbulence resulting from the interaction between the water base morphology and strong tidal currents.

3.6 Oceanographic parameters as indicators of RoFI conditions

The results of the (PCA) based on CTD data from various observation stations in the Musi-Banyuasin Estuary are shown in **Fig. 10**. The first principal component (PC1) accounted for 55.79% of the total variance, whereas the second principal component (PC2) explained 24.35%, capturing 80.13% of the overall data variability.

The dominance of seawater in PC1 (F1) was marked by very strong positive correlations with salinity (0.981), Sigma-T (0.988), and conductivity (0.931) (**Table 3**). Similarly, the eigenfactor values shown in **Table 2** indicate that the parameters temperature, salinity, and TSS have a strong relationship. The variable contribution data in **Table 4** confirms this, where Sigma-T and Salinity contribute the most to F1, at 21.890% and 21.576%, respectively. This condition reflects the characteristics of the water mass at the outer estuary stations (P9–P14) during high tides. Conversely, at the inner stations (S1–S8) during the ebb tide, the influence of river flow and sediment becomes more prominent through PC2 (F2). The Turbidity parameter showed the highest loading factor of 0.901 for F2, followed by chlorophyll-a (0.700), and TSS (0.669). This is supported by **Table 4**, which shows that turbidity contributed 41.668% to the variability in F2. The negative relationship between these parameters and salinity and conductivity in PC1 confirmed the existence of a dynamic water mass exchange. Temperature also played an important role, with a dominant contribution of 41.485% to F3, which reinforces the understanding of vertical mixing and RoFI dynamics in this estuarine region.

Table 2. The eigenfactors matrix water quality parameters shows the relative weight or score coefficient of each parameter in the formation of each principal component (F1–F5).

Parameters	F1	F2	F3	F4	F5
Temperature (°C)	-0.356	-0.052	0.644	-0.408	-0.402
Salinity (PSU)	0.464	0.079	0.071	0.057	0.081
Conductivity (mS/cm)	0.441	0.128	0.195	0.084	-0.307
SigmaT (σ_t)	0.468	0.050	0.020	0.041	-0.003
Chlorophyll-a (µg/L)	-0.166	0.502	-0.631	-0.334	-0.367
Turbidity (FTU)	-0.070	0.646	0.286	-0.231	0.649
DO (%)	0.394	0.272	0.156	-0.303	-0.321
TSS (mg/L)	-0.238	0.479	0.191	0.752	-0.282

Table 3. The factor loadings (variable correlation with factors) displays the correlation values between the original variables and the main factors.

Parameters	F1	F2	F3	F4	F5
Temperature (°C)	-0.752	-0.073	0.561	-0.273	-0.174
Salinity (PSU)	0.981	0.110	0.062	0.038	0.035
Conductivity (mS/cm)	0.931	0.179	0.170	0.056	-0.133
SigmaT (σ_t)	0.988	0.070	0.017	0.028	-0.001
Chlorophyll-a (µg/L)	-0.350	0.700	-0.550	-0.224	-0.159
Turbidity (FTU)	-0.147	0.901	0.249	-0.155	0.282
DO (%)	0.833	0.380	0.136	-0.203	-0.139
TSS (mg/L)	-0.503	0.669	0.167	0.504	-0.123

Table 4. The percentage contribution of variables to factors explains the proportion (%) of contribution of each parameter in explaining the variability in each factor.

Parameters	F1	F2	F3	F4	F5
Temperature (°C)	12.655	0.272	41.485	16.609	16.122
Salinity (PSU)	21.576	0.620	0.504	0.320	0.652
Conductivity (mS/cm)	19.431	1.638	3.809	0.698	9.449
SigmaT (σ_t)	21.890	0.248	0.040	0.169	0.001
Chlorophyll-a (µg/L)	2.743	25.182	39.874	11.137	13.452
Turbidity (FTU)	0.484	41.668	8.177	5.321	42.082
DO (%)	15.545	7.409	2.447	9.181	10.275
TSS (mg/L)	5.675	22.962	3.664	56.565	7.967

During the flood tide, particularly at the outer estuary stations (P9–P14), seawater predominates, characterized by higher salinity, conductivity, and density values, all of which show positive correlations in PC1. During ebb tide, especially at the inner estuary stations (S1–S8), TSS, turbidity, temperature, and chlorophyll-a increased, showing positive correlations with one another due to river runoff and sediment resuspension. However, these parameters are negatively correlated with salinity and conductivity, both of which decline when the freshwater input dominates. Such conditions enhance vertical mixing and strongly influence the RoFI dynamics in the Musi-Banyuasin estuary. Meanwhile, at the outer estuary stations (S9–S14), although seawater influence persisted, salinity values were lower than during flood tide, indicating more intense mixing between freshwater and seawater.

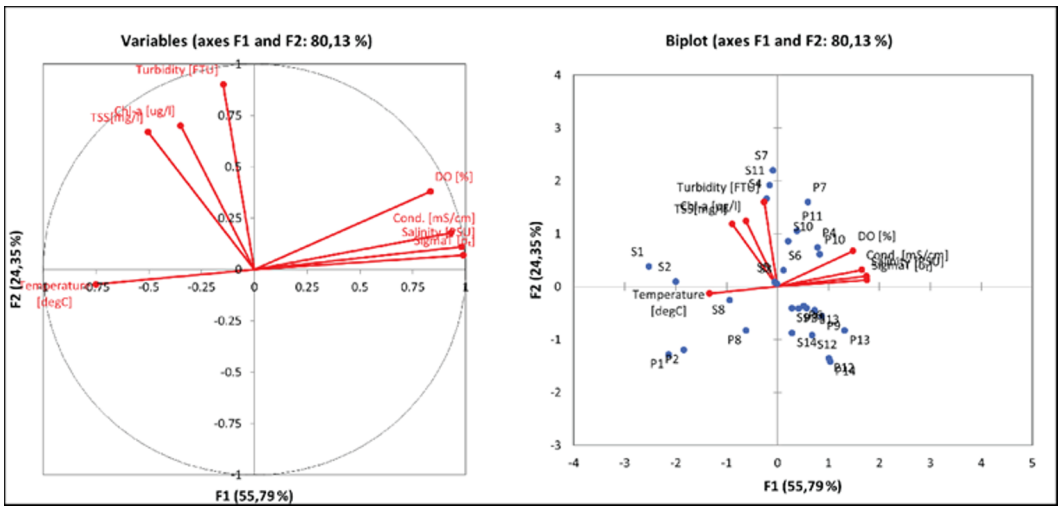

Fig. 10. The results of the principal component analysis of several oceanographic parameters characterize the RoFI conditions at the Musi-Banyuasin Estuary during the rising and falling tides on axis 1 (F1) and axis 2 (F2).

4 Conclusion

Salinity distribution in the RoFI region is controlled by complex interactions between estuarine morphology, current patterns, river discharge, and tidal dynamics, where the ebb phase produces current velocities of approximately 0.2 m/s toward the mouth, while the flood phase drives the intrusion of seawater (28–30 PSU) that meets with low-knowledge turbid river water (5 PSU). Although this study successfully identified the physical mechanisms underlying the formation of a dynamic mixing zone in accordance with the research

objectives, this investigation has limitations in the short observation time span, and thus does not capture long-term variability.

Therefore, further research should include cross-seasonal observation periods to gain a comprehensive understanding of the temporal dynamics of estuaries. Overall, the results of this study provide a crucial basis for predicting primary productivity and pollutant risk, which ultimately clarifies the hydrodynamic constraints for maintaining ecological balance and water quality in estuarine environments.

References

1. A. Agussalim, S.H. Murti, L.W. Santosa, Determining spatio-temporal distribution dynamics of chlorophyll-a in Banyuasin sea waters using remote sensing data in Proceedings of the Eight Geoinformation Science Symposium 2023, Geoinformation Science for Sustainable Planet, Yogyakarta, Indonesia, August 28-30 (2023), 129770U. https://doi.org/10.1117/12.3009669
2. L. Ross, S. Alahmed, S.M.C. Smith, G. Roberts, Tidal and subtidal transport in short, tidally-driven estuaries with low rates of freshwater input. Continental Shelf Researc. **224**, 104453 (2021). https://doi.org/10.1016/j.csr.2021.104453
3. C. Pao, A. Romdani, J. Chen, Tidally-modulated stratification in a channel-shoal estuary. Estuarine, Coastal and Shelf Science. **284**, 1–12 (2023). https://doi.org/10.1016/j.ecss.2023.108279
4. J.L. Hassrick, J. Korman, W.J. Kimmerer, E.S. Gross, L.F. Grimaldo, C. Lee, A.A. Schultz, Freshwater flow affects subsidies of a copepod (*Pseudodiaptomus forbesi*) to low-salinity food webs in the upper San Francisco estuary. Estuaries and Coasts. **46**, 450–462 (2023). https://doi.org/10.1007/s12237-022-01142-1
5. X. Zhang, J. Huang, J. Chen, Y. Zhao, Remote sensing monitoring of total suspended solids concentration in Jiaozhou Bay based on multi-source data. Ecological Indicator. **154**, 110513 (2023). https://doi.org/10.1016/j.ecolind.2023.110513
6. Z. Safar, C. Chassagne, S. Rijnsburger, M.I. Sanz, A.J. Manning, A.J. Souza, T.V. Kessel, A. Horner-Devine, R. Flores, M. McKeon, *et al*. Characterization and classification of estuarine suspended particles based on their inorganic/organic matter composition. Front. Mar. Sci. **9**, 1–14 (2022). https://doi.org/10.3389/fmars.2022.896163
7. N. Durand, A. Fiandrino, P. Fraunié, S. Ouillon, P. Forget, J.J. Naudin, Suspended matter dispersion in the Ebro ROFI: An integrated approach. Continental Shelf Research. **22**, 267–84 (2002). https://doi.org/10.1016/S0278-4343(01)00057-7
8. J.C. Dauvin, E. Thiébaut, Z. Wang, Short-term changes in the mesozooplanktonic community in the Seine ROFI (Region of Freshwater Influence) (eastern English Channel). J. Plank. Res. **20**, 1145–67 (1998). https://doi.org/10.1093/plankt/20.6.1145
9. R. Kopte, M. Becker, P. Holtermann, C. Winter, Tides, stratification, and counter rotation: The German Bight ROFI in comparison to other regions of freshwater influence. J. Geophys. Res.: Oceans. **127** (2022). https://doi.org/10.1029/2021JC018236
10. D. Salas-Monreal, O. Avendaño, J. de Jesus Salas-Perez, M. Marin-Hernandez, Surface flow modulation by river discharges in a tropical micro-tidal estuary. Estuarine, Coastal and Shelf Science. **286** (2023). https://doi.org/10.1016/j.ecss.2023.108339
11. S. Querin, A. Crise, D. Deponte, C. Solidoro, Numerical study of the role of wind forcing and freshwater buoyancy input on the circulation in a shallow embayment

(Gulf of Trieste, Northern Adriatic Sea). J J. Geophys. Res.: Oceans. **112**, 1–19 (2007). https://doi.org/10.1029/2006JC003611

12. A. Loveridge, K.A. Pitt, C.H. Lucas, J. Warnken, Extreme changes in salinity drive population dynamics of Catostylus mosaicus medusae in a modified estuary. Mar. Environ. Res. **168** (2021). https://doi.org/10.1016/j.marenvres.2021.105306
13. M.A. Janout, J. Hölemann, G. Laukert, A. Smirnov, T. Krumpen, D. Bauch, L. Timokhov, On the variability of stratification in the freshwater-influenced Laptev Sea Region. Front. Mar. Sci. **7**, 543489 (2020). https://doi.org/10.3389/fmars.2020.543489
14. D. Fugate, F. Jose, Forces in an estuary tides, freshwater, and friction. Oceanography. **32**, 231–6 (2019). https://doi.org/10.5670/oceanog.2019.105
15. J. Xing, S. Chen, A process study of the interaction of tidal currents, tidal mixing and density gradients in a region of freshwater influence. Journal of Marine Systems. **172**, 51–63 (2017). https://doi.org/10.1016/j.jmarsys.2017.02.008
16. M.S. Montalvo, E. Grande, A.E. Braswell, A. Visser, B. Arora, E.C. Seybold, C. Tatariw, J.C. Haskins, C.A. Endris, F. Gerbl, et al. Correction : A fresh take: seasonal changes in terrestrial freshwater inputs impact salt marsh hydrology and vegetation dynamics. Estuaries and Coasts. **47**, 2714 (2024). https://doi.org/10.1007/s12237-024-01413-z
17. A.M. Hoguane, T. Gammelsrød, S. Mazzilli, M.H. Antonio, N.B.F. da Silva, The hydrodynamics of the Bons Sinais Estuary: The value of simple hydrodynamic tidal models in understanding circulation in estuaries of central Mozambique. Regional Studies in Marine Science. **37**, 101352 (2020). https://doi.org/10.1016/j.rsma.2020.101352
18. H. Surbakti, I.W. Nurjaya, D.G. Bengen, T. Prartono, Temporal variation of freshwater as control of mangrove in Banyuasin Estuary, South Sumatra, Indonesia. J Biol. Div. **24**, 3 (2023). https://doi.org/10.13057/biodiv/d240320
19. S. Heltria, I.W. Nurjaya, J.L. Gaol, Turbidity front dynamics of the Musi Banyuasin Estuary using numerical model and Landsat 8 satellite. AACL Bioflux. **14**, 1–13 (2021)
20. M.M. Baustian, F.R. Clark, A.S. Jerabek, Y. Wang, H.C. Bienn, E.D. White, Modeling current and future freshwater inflow needs of a subtropical estuary to manage and maintain forested wetland ecological conditions. Ecological Indicatorst. **85**, 791–807 (2018). https://doi.org/10.1016/j.ecolind.2017.10.005
21. S.K. Niveditha, C.K. Haridevi, R. Hardikar, A. Ram, Phytoplankton assemblage and chlorophyll a along the salinity gradient in a hypoxic eutrophic tropical estuary-Ulhas Estuary, West Coast of India. Marine Pollution Bulletin. **180**, 113719 (2022). https://doi.org/10.1016/j.marpolbul.2022.113719
22. I. Martins, P. Maranhão, J.C. Marques, Modelling the effects of salinity variation on Echinogammarus marinus Leach (Amphipoda, Gammaridae) density and biomass in the Mondego estuary (Western Portugal). Ecological Modelling. **152**, 247–60 (2002). https://doi.org/10.1016/S0304-3800(02)00012-1
23. A. Wodeyar, S. Akter, S. Nama, P. Gogoi, K. Ramteke, P. Layana, B.B. Nayak, A.T. Landge, G. Deshmukhe, A.K. Jaiswar, Decoding the dynamics of potentially Harmful Algal Bloom (HAB) species, environmental influences and shellfish toxicity in a tropical mesotidal estuary. Mar. Pollut. Bull. **215**, 117845 (2025). https://doi.org/10.1016/j.marpolbul.2025.117845
24. I. Setiawan, Y. Haditiar, M. Syukri, N. Ismail, S. Rizal, Suspended sediment transport generated by non-hydrostatic hydrodynamics in Northern Waters of Aceh, Indonesia.

Heliyon. **9**, e17367 (2023). https://doi.org/10.1016/j.heliyon.2023.e17367

25. L. Maslukah, A. Wirasatriya, E. Indrayanti, H.N. Krisna, Estimation of chlorophyll–a and total suspended solid based on observation and Sentinel-2 imagery in coastal water Teluk Awur, Jepara-Indonesia. Int. J. Geoinformatics. **19**, 18–27 (2023). https://doi.org/10.52939/ijg.v19i8.2777